

**GT2011-46552**

## **BOUNDARY LAYER CONTROL FOR A VERTICAL AXIS WIND TURBINE USING A SECONDARY-FLOW PATH SYSTEM**

### **Alexandrina Untaroiu**

Mechanical and Aerospace Engineering  
University of Virginia  
Charlottesville, VA, USA  
au6d@virginia.edu

### **Houston G. Wood**

Mechanical and Aerospace Engineering,  
University of Virginia  
Charlottesville, VA, USA  
hwood@virginia.edu

### **Archie Raval**

Mechanical and Aerospace Engineering  
University of Virginia  
Charlottesville, VA, USA  
aar3v@virginia.edu

### **Paul E. Allaire**

Mechanical and Aerospace Engineering,  
University of Virginia  
Charlottesville, VA, USA  
pea@virginia.edu

### **ABSTRACT**

Vertical axis wind turbines (VAWTs) have typically lower efficiency compared to their horizontal counterparts (HAWTs), but are attractive for places where taller structures are prohibited, as well as for regions where available wind speeds are lower. For HAWTs, the blades are always perpendicular to the incoming wind, providing a continuous thrust throughout the rotation. Contrary to HAWTs, VAWTs have advancing blades and retreating blades, where blades backtrack against the wind, causing lower efficiency. Hence, any modifications that can be made to improve the efficiency of VAWTs can be beneficial to the wind industry. Passive flow control permits the airfoil geometry to be modified by means of grooves or slots without requiring heavy mechanisms or actuators. Hence, this form of boundary layer control seems advantageous for wind turbines, so that minimal amount of maintenance is required, while complexity of the turbine is not significantly increased. Such modification changes the boundary layer over an airfoil reducing flow separation and reversed flow. This study introduces a new form of passive flow control: Secondary-flow control system, which works on the principle of mass removal, eliminating flow separation at different apparent angles of attack in a VAWT. CFD analysis is used to investigate passive flow control for the airfoils NACA8H12 and LS0417 in a three-bladed VAWT configuration. A secondary flow path is initially designed and optimized in a single airfoil configuration, and then used to adjust the wind turbine blade design. The effects of secondary-flow control system in a VAWT design configuration are investigated by

comparison with the non-modified airfoil design. The CFD results indicate that secondary-flow path system can be used to modify and control the boundary layer for a wind turbine. It is believed that secondary-flow control system incorporated in VAWT design has potential for improving turbine efficiency. Further research should be conducted to optimize the secondary-flow path system according to the shape of the airfoil in a 3D VAWT configuration, so that blades interference can be captured.

### **INTRODUCTION**

Flow separation tends to occur when the fluid boundary layer travels against the adverse pressure gradient, wherein, the speed of the boundary layer becomes close to zero, characterized by stall conditions [1-4]. At higher angles of attack, the flow reverses its direction and starts moving back upstream. This reversed flow causes flow separation and recirculation of flow downstream. The inflection point where the flow starts to reverse typically occurs after the separation point [4]. In a vertical axis wind turbine, each blade is subjected to a different apparent angle of attack. While the angle of attack on the advancing blade might be optimal, the retreating blades have higher angles of attack and a tremendous amount of lift is lost. Secondary flow control system, which works on the principles of mass removal can therefore, eliminate the flow separation that is caused by higher incident angles. If mass can be removed before the separation point or inflection point, separation can be delayed. This manipulation of flow is referred to as flow control.

The concept of flow control dates back as early as in 1904, when Prandtl pioneered the modern use of flow control [2]. Prandtl introduced the boundary layer theory and described several experiments in which boundary layer could be manipulated/controlled. During the Second World War, extensive research was done on laminar flow control, wherein the boundary layer formed along the external surfaces of an aircraft was controlled and suction was used as a means to delay transition on a swept wing of X-21 [2]. The oil crisis of 1970s renewed interest in boundary layer control to reduce skin friction drag especially in turbulent regions [2].

Previously, flow control has been achieved on airfoils using two types of flow control, Active and Passive flow control, which are briefly reviewed below.

### Active Flow Control

Active flow control includes actuators and external mechanisms to introduce/eliminate/modify flow according to the need. These mechanisms typically work by controlling Reynolds numbers ( $Re$ ), Mach number ( $Ma$ ) or pressure to remove from the boundary layer and re-ingesting the flow in it later. Active flow control “manipulates a flow field by using a time dependent forcing system, typically to leverage a natural instability of the flow and thus to amplify the control effectiveness” [3]. There are various techniques that have been developed by the researchers to delay the onset of separation or to control flow.

Most of the previous research done on flow control has typically been done on airfoils only, which are adapted to airplanes.

Periodic excitation is one such active flow control system that prevents flow in an undesired direction by controlling conditions like Reynolds number, Mach number, introducing pressure gradients and modifying surface geometry by introducing a steady momentum or removing mass from the boundary layer [5]. “Control or actuation can be achieved by surface mounted or cavity installed zero-mass flux actuators, capable of delivering sufficient amplitudes for effective control” [5]. Seifert et al. [5], showed in their experiment that the periodic excitation that is generated by actuators has been more effective than introducing fluids in the boundary layer by means of blowing as a means of flow control. Figure 1 represents the excitation slot experiment on the airfoils.

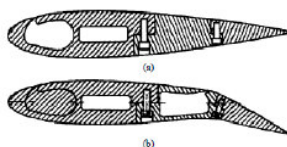


Figure 1. Geometric representation of the excitation slot at a) 0.1c and b) 0.3 c

Blowing at the leading edge has also been considered for active flow control. However, it has been shown to have worse results than the baseline case [6]. Leading edge blowing

creates greater circulation around the separation bubble and the flow is further detached.

In numerous studies, leading edge suction is used to delay separation. These methods create suction at the leading edge and blowing at the trailing edge using oscillatory motions and excitation frequency, which has been found to be more effective than steady blowing air [6]. The Figure 2 below shows an unsteady wall jet dispersed from the slotted flap closer to the leading edge [6]. This jet excited the flow and delayed separation and reattachment.

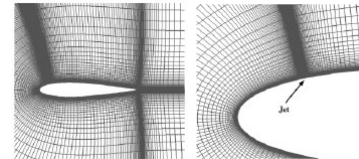


Figure 2. Computational grid for flow control

Huang et.al [7], proved that when the suction is perpendicular to the leading edge, higher lift is produced. This study also showed that blowing is more favorable when it is tangential downstream. Figure 3 below, shows the reduction in bubble separation at each jet location and the favorable location for suction and blowing.

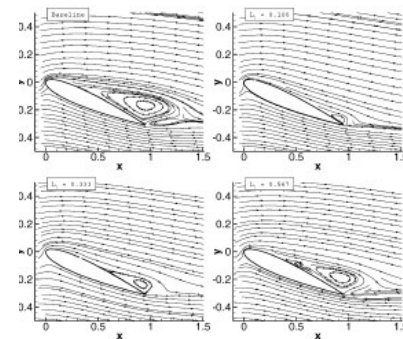


Figure 3. Bubble separation at each jet location

The concept of flow control has also been applied to the field of gas turbines. In the study by Lord et al. [3], small modifications through fluid injections are made to change the behavior of the flow. Active compressor stability control has been one of the most beneficial flow control applications in the gas turbine industry. “The current approach avoids stall by scheduled bleed and stator vane actuation” [3]. Feedback can thereafter be utilized to stabilize the unstable dynamics.

### Passive Flow Control

While active flow control needs actuators, passive flow control does not require any such external mechanisms. It includes the mechanisms as a part of the geometry. This ensures that the system is simple and not complicated with actuator controlled mechanisms. It eliminates any extra weight caused by heavy mechanisms and reduces maintenance and repair related costs [8]. There are various passive flow control

means utilized on airfoils so far, such as drooped airfoils, porosity, s-ducts and many more.

Variable Droop Leading Edge Airfoil is a passive flow control mechanism used customarily in a helicopter rotor. “Drooping the leading edge substantially modifies the airfoil pressure distributions such that the dynamic stall onset mechanisms is changed from shock-induced to pressure gradient induced for certain flow conditions” [8]. This method employs large sinusoidal motion that alters cyclic pitch. Figure 4 shows the drooped airfoils b) and c) as compared to the non-drooped airfoil a). This method has proven to have controlled dynamic stall flow by drooping the leading edge and simulating pitching oscillations at the same time.



Figure 4. a) Undrooped airfoil. b) and c) Drooped VR-12 airfoils

Aerospace industry imports a lot of flow technology from fishes and amphibian mammals, by inspecting the movements of these creatures in water [9,10]. Swimming fishes and mammals also demonstrate active and passive flow control mechanisms, with passive mechanisms relying on the structural and morphological components of the body, such as riblets, fin-modifications or hump back whale tubercles [9]. Figure 5 shows a picture of the structural components of a whale’s fin, which inspire flow control. Flow control mechanisms in these creatures is in the form of appendage usage or using body musculature to generate wake flow structures or stiffening fins against hydrodynamic loads [9]. Fish can actively control fin curvature, displacement and area as well.

The humpback whale flipper has rounded protuberances or tubercles on the leading edge. “The position and number of tubercles on the flipper suggested analogues with specialized leading edge control devices associated with improvements in hydrodynamic performance suggested that humpback tubercles may reduce drag due to lift on the flipper” [9]. Various biological wings utilize leading edge control devices to control lift and avoid stall at high angles of attack and low speeds.



Figure 5. a) Tubercles of a hump back whale b) structural components c) control devices associated

Like fish and aquatic animals, birds have also been studied to develop various technologies in the aerospace industry. The research done by Favier et al [11], explores the self-adaptation

of a birds’ wing to the separated flow during landing. The model of hairy coating resembling feather-like qualities is developed and the fluid around the hairy coating is analyzed by means of numerical simulation. The study found that the hairy coating was “capable of increasing global aerodynamic performances of an immersed body, by adapting to the separated flow” [11].

Another attempt at controlling the flow passively has been made using porous medium. The new passive control strategy used in the study of implementing a “porous layer between a bluff-body and a fluid, in order to change the boundary layer characteristics,” [12] gave drastic results for higher Reynolds numbers. This study proved that the passive flow control methods can be equally fruitful.

The research by Bridges [13] tested the effects of application of different suction zones with holes placed experimentally throughout the airfoil. The transition occurred before the porous area. In this study, trailing edge suction was found to have a more considerable effect reducing separation and profile drag in an airfoil, with the tip of the wing acting naturally as a suction source due to low pressure profile.

Hence, a lot of research has been done in the field of flow control, active and passive and both forms of flow control are promising on an airfoil. While research has been done to adapt flow control on most forms of aerospace technology, application of flow control to wind turbines has targeted primarily HAWT and was mostly focused on active flow control methods [14-25].

In order to address this research gap, this study considers VAWT and is aimed to investigate a new form of passive flow control system named Secondary Flow Control (SFC) system. Instead of having constant suction and blowing actively using actuators, a secondary flow path (SFP) is designed, which takes in the air at the leading edge and channels it through the trailing edge. This SFC system is proposed to delay separation, reduce separation bubbles and to modify/control the flow path. Two airfoils are analyzed with and without this system in a wind turbine configuration to check for flow modification and control.

## FLOW CONTROL APPLIED TO WIND TURBINES

With an increased need for alternate resources, wind turbines have been gaining popularity. As illustrated in Figure 6, there are two types of wind turbines that are lift-based: HAWTs and VAWTs.

HAWT rotates about a horizontal axis, with the blades always being perpendicular to the incoming wind. They are equipped with yaw systems in order to position themselves against the wind. This produces constant torque and provides a better efficiency. HAWT typically has tall towers and gets better wind speed advantage because of its altitude. However, tall towers tend to be heavier, with the blades itself being 45m, which adds a challenge to the transportation and installation. Moreover, the generator and gear box have to be housed near the blades, adding to the weight.

In contrast, the rotational axis of a VAWT is perpendicular to the incoming wind. Because this is true regardless of the direction from which the wind enters, no yawing mechanism is necessary. The gearbox and generator are typically mounted on the ground below the rotor, thus cutting down the weight. Vertical axis wind turbines require low start up speed and are suitable for places where wind velocity is low.



Figure 6. Wind turbine: a) VAWT and b) HAWT

Differences between the HAWT and VAWT configurations result in a number of pros and cons [26]. First, because no yawing mechanism is needed in the VAWT, construction is simpler. Moreover, there is no chance of misalignment with the incoming wind, as occurs in extremely large HAWTs whose orienting systems cannot respond quickly enough to wind changes. This simplicity is echoed in the VAWT blade manufacture, which is generally comprised of a simple constant cross-sectional extrusion. In contrast, HAWT blades usually include both twist and pitch. Maintenance and repairs in the VAWT are easier because the generator and gearbox are located at or near ground level. This affords an opportunity to acoustically insulate them, resulting in a decrease in mechanical noise. VAWTs also typically operate at lower wind speeds, making them aerodynamically quieter. This slower speed, along with increased visibility, results in far fewer wildlife collisions, a major criticism of older HAWT farms [27].

In spite of these features, VAWTs have lagged considerably in development and implementation compared to their HAWT counterparts. The commercial wind turbine industry largely focused on massive HAWTs, which have become standard in power production. Passive techniques improve the turbine's performance and/or reduce loads without external energy expenditure. However, since the beginning of the commercial wind industry, there was a tendency of increasing the rotor diameter and turbine size to reduce the cost of energy produced. Significant growth of HAWT size and weight over the past few decades required implementation of active flow control and has made it impossible to control turbines passively as they were controlled in the past. Methods of active control are rotor yaw, blade pitch, variable-speed rotor, microtabs, trailing-edge flaps, and synthetic jets [14].

One of the biggest disadvantage of a VAWT is its' reduced efficiency. Since blades are not always perpendicular to the oncoming wind, only one or two blades are advancing and others backtrack against the wind reducing the efficiency.

Hence, any improvements that can be made to the VAWTs would be beneficial to the wind industry and especially for places with lower wind speeds. As an example, the state of Virginia typically gets 15mph of winds which are variable. Hence, this type of wind turbine is better suited to the location.

One of the primary concerns for a wind turbine is the amount of maintenance required. Active flow control almost always requires maintenance/repair of actuators and synthetic jets. No previous research has been done on using secondary flow paths or passive flow control means to optimize the performance of a VAWT, hence most of our research is based on the studies done on an airplane wing. After careful review of the previous research done, passive flow control of the airfoil was chosen. This control mechanism has been selected to simplify the experiment and to incorporate any flow control features into the geometry without adding to the cost of wind turbine manufacture. While active flow control seems promising, it requires actuators with a precise actuation control. Taking into consideration the previous research done in the field of helicopter rotors, aquatic animals and airplanes, a form of passive flow control is introduced in this study called secondary flow path system (Figure 7). The initial concept of secondary flow path for lift increase was first time proposed in 1935 [28].



Figure 7. Conceptual Design of secondary flow path system with inlet at leading edge, outlet at 85% chord

Research has shown that having suction on leading edge and blowing at trailing edge is beneficial [7]. The current mechanism takes into account the suction and blowing method used by synthetic jets and channels flow like an s-duct, however, it is implemented as a passive means by designing the geometry with this secondary flow path system.

## METHODOLOGY

The main idea of this study was to design a secondary flow path through a turbine blade that creates a natural suction through pressure gradient and channel some of the flow through the SFC system and reintroduce it at the trailing edge after flow separation occurs. The standard airfoil and the airfoil modified by incorporating a secondary flow path were evaluated on a vertical axis wind turbine configuration. This study investigates if the reduction in flow separation is considerable for the secondary flow control system. The proper configuration of the secondary flow path that was applied to the turbine blade was selected based on a CFD study that is summarized below.

### Airfoil with Secondary Flow Path Design Concept

In order to be able to apply SFC system on wind turbines, a two-dimensional study with different secondary flow control

systems was performed on the airfoil LS0417. For this study, the locations of SFC system were investigated, one starting at the leading edge running parallel to the trailing edge; and one at a certain  $x/c$  location along the chord to the trailing edge (Figure 8).

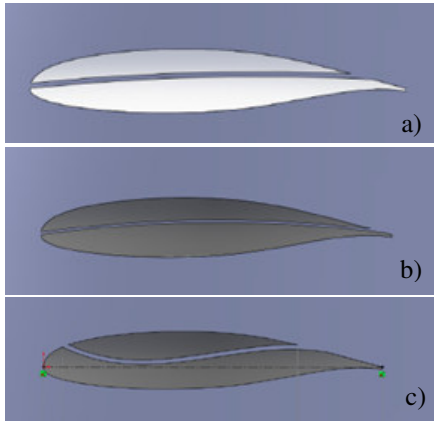


Figure 8. Different SFC flow paths investigated; a) has flow inlet at the leading edge and exit at 75% $c$  and thickness of 0.033ft; b) has flow inlet at the leading edge and exit at 75% $c$ , however the thickness is 0.01667 ft; and c) has flow inlet at the quarter chord and flow exit at 75%  $c$

### Vertical Axis Wind Turbine Configurations

In order to investigate the difference made by SFC system, two airfoils, LS0417 and NACA8H12, were used in the wind turbine configuration illustrated in Figure 9. This figure shows the prototype of University of Virginia’s vertical axis wind turbine and the cross sectional view. Both airfoils selected are non-symmetric, to give a better lift coefficient.

Figure 10 and 11 show these two airfoils with standard airfoil configuration and with SFP control system, respectively. The blade with standard airfoil is defined as baseline and the one with SFP is referred to as modified blade configuration. The SFP selected for this study has flow inlet at the leading edge, exit at 75% $c$  and thickness of 0.033ft (Fig.8a).

The vertical axis wind turbine has three blades, with a hub radius of 0.0635 m, spar of 0.2667 m, and rotor outer diameter of 0.796 m. The wind tunnel, where the turbine prototypes are intended to be tested, is 1.524m by 3.048 m (5x10 ft), therefore, these dimensions were employed to define the outer domain encompassing the turbine’s model. The incoming wind speed considered is 6m/s. The turbine rotates at 700 rpm, which correspond to a tip speed ratio of approximately 4. Table 1 lists the model parameters for VAWT.

**Table 1.** UVA Vertical Axis Wind Turbine- Model Parameters

|                         | LS0417 | NACA8H12 |
|-------------------------|--------|----------|
| blade airfoil chord [m] | 0.3048 | 0.3048   |
| hub radius [m]          | 0.0635 | 0.0635   |
| spar length [m]         | 0.2667 | 0.2667   |
| blade span [m]          | 3.2    | 3.2      |
| number of blades        | 3      | 3        |

From the previous study of the airfoil LS0417 described above, it was found that the SFC system with inlet at the leading edge and outlet at the trailing edge was very beneficial in removing the mass flow as it did not re-ingest the air flow in a manner which further created re-circulation. Hence, the SFC system with inlet at the leading edge was used in the comparison for wind turbine configuration.

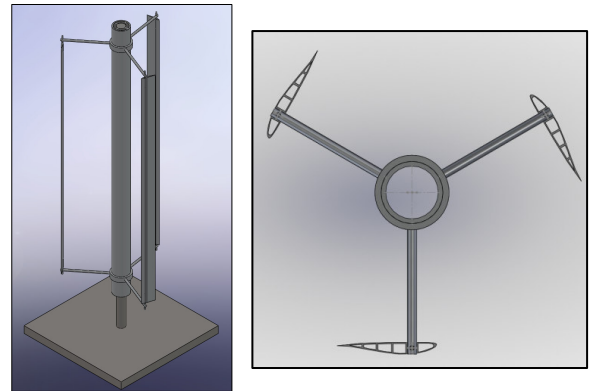


Figure 9. a) UVA Turbine Prototype and b) cross- section intersecting the spars

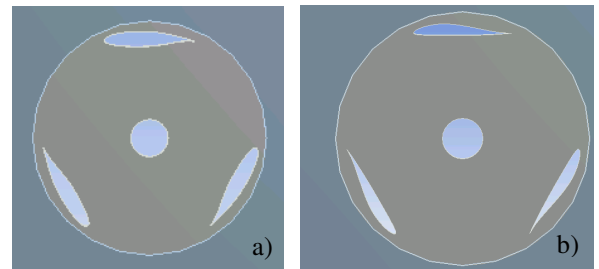


Figure 10. Turbine with Standard Airfoil Configuration (Baseline); a) LS0417 and b) NACA8H12

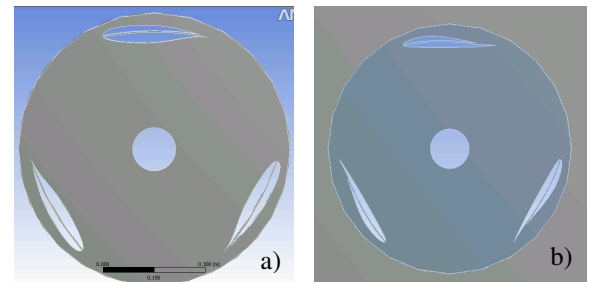


Figure 11. Turbine with SFP Control System (Modified) a) LS0417 and b) NACA8H12

### Numerical Modeling Approach

Transient CFD simulations were performed using a commercially available CFD package, ANSYS CFX ( ANSYS Inc, Canonsburg, PA). Calculations were performed based on solving the Reynolds Averaged Navier Stokes (RANS) equations. The SST  $k-\omega$  turbulence model combined with Gamma Theta transition model was used for turbulence modeling. The sections below provide the details for the computational models and boundary conditions employed.

**Computational Models** For the purpose of this study, an unstructured type of mesh was generated in Ansys in order to replicate the physics of the problem. Therefore, the parameters listed in Table 1 and 2 were incorporated into 3D CFD models where blade height was set to 1 in. The mesh around the airfoils was refined and inflation layers, radiating from the surface of the airfoils, were applied to capture the boundary layer details (Figure 12, 13). The number of grid elements for each model, the resultant of a grid convergence study, is listed in Table 3.

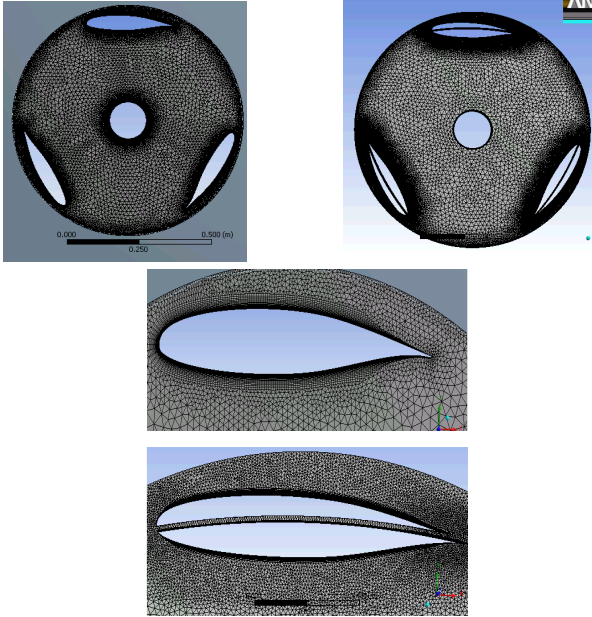


Figure 12. Mesh for LS0417, baseline and modified configuration; and detail view

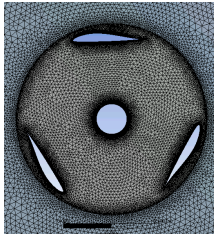


Figure 13. Mesh for NACA8H12 baseline, showing both outer and inner rotating domain

**Table 2.** Computational Models and Parameters

| Models with and without secondary flow path |            | LS0417 | NACA8H12 |
|---|------------|--------|----------|
| Outer domain                                | length [m] | 3.048  | 3.048    |
|   | width [m]  | 1.524  | 1.524    |
|   | height [m] | 0.0254 | 0.0254   |
| Inner domain containing the turbine blades  | radius [m] | 0.398  | 0.398    |
|   | height [m] | 0.0254 | 0.0254   |

**Table 3.** Mesh Parameters

|  | Single airfoil model  | Wind Turbine Models   |
|--|-----------------------|-----------------------|
| Number of grid elements with and without SFC | ~200k<br>~3.6 million | ~800k<br>~5.4 million |

## Boundary Conditions

**Single blade configuration** For selection of secondary flow path, a single airfoil configuration was considered. The domain was set as stationary. The incoming wind direction of 6 m/s was altered to correspond to 25 degree angle of attack to ensure that the flow is not only separated by also recirculating.

**Wind turbine models** For this set of simulations, the computational domain was split in two parts, a circular inner domain containing the blades and a rectangular outer domain (Figure 14b) [17]. The two domains, one rotating and one stationary, were attached through a transient rotor-stator interface. The circular domain, specified in a rotating frame of reference, spins with 700 rpm. In the transient simulations, the blades were set to rotate in one degree increment per time step. Thus, the corresponding time step specified was  $t = 2.3810E-04$  seconds. A maximum number of 10 iterations was selected for each time step. The residual target for the convergence criteria was the root mean square (RMS) normalized value of  $1e-05$ .

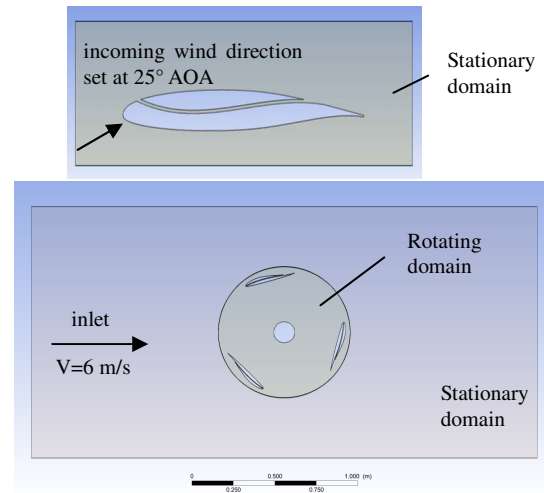


Figure 14. Computational Models and Boundary Conditions Setup a) Single airfoil set up b) wind turbine configuration

The rotor is the section with the hub and airfoils at radial location from the hub. The flow through the wind turbine is modeled as if it were in a wind tunnel section. Both the airfoils were issued to the same boundary conditions to be able to create proper comparison. The incoming wind was set to 6 m/s, which was specified as inlet condition, whereas

atmospheric pressure is set as outlet boundary condition. The top and the bottom of the stator were treated as symmetry surfaces.

## RESULTS AND DISCUSSION

Two types of simulations were performed. One analyzed a single airfoil with different SFC flow paths to compare and select an optimal SFC flow path and the second type analyzed this SFC in a vertical axis wind turbine configuration. This dual simulation approach was intended to validate the passive flow control concept proposed.

### Secondary Flow Path Design Concept

The SFC flow path for wind turbine model configuration was selected after investigating different flow paths in a 3-D set up with just a single airfoil, stationary domain and incoming wind direction at 25 degree AOA. The purpose of the single blade configuration was to test the introduction of SFC in a simpler setting, to be able to validate the design concept. The main idea of this initial study was to design a secondary flow path through the airfoil that creates a natural suction through pressure gradient and channel some of the flow through the SFC system and reintroduce it at the trailing edge after flow separation occurs. Hence, the first SFC system analyzed, started at leading edge and ran parallel to the trailing edge, whereas the second SFC system inlet was at 5.64% chord and the outlet was at 75% chord. For different flow paths tested, Figure 15 below shows the streamlines starting from the inlet boundary and are colored according to magnitude of velocity. Figure 15.a) illustrate the airfoil with no Secondary Flow path, Fig 15.b) has flow inlet at the quarter chord and flow exit at 75%c, whereas Figure 15.c) and d) have flow inlet at the leading edge and exit at 75%c and thickness of 0.033ft and 0.0166 ft respectively.

Point of inflection is a point where the flow begins to travel against the pressure gradient. This point occurs beyond the separation point. The separation on the surface occurs at  $dv/dn=0$ , where  $v$  is the velocity in the direction tangential to the flow and  $n$  is a similarity variable characterized by  $y$  distance of the flow divided by the boundary layer thickness [1]. Hence, placing the insertion point of the SFP at the leading edge, upstream the separation point and inflection point, will guarantee delayed separation and reduced separation bubble. Due to this effect, the SFC flow path considered in Figure 15 b) added further separation and re-circulation. As compared to the airfoil with no SFC flow path shown in Figure 15a), the airfoil with inlet at 0.25c displays massive flow separation. In airfoil with no SFC, recirculation starts to occur at the trailing edge of the airfoil. After introducing SFC system at leading edge (Fig. 15c), this re-circulation is greatly reduced and the flow is made more streamlined. This study also tested the thickness of the SFC system of 0.033ft and 0.0166 ft. Having a thicker SFC system, thicker than 0.1 ft, would result in a massive re-introduction of the flow at the trailing edge, which would further introduce more circulation. However, SFC

system thickness less than 0.01 ft would not remove enough mass flow for the SFC system to work. Hence, two thicknesses were selected to meet this requirement.

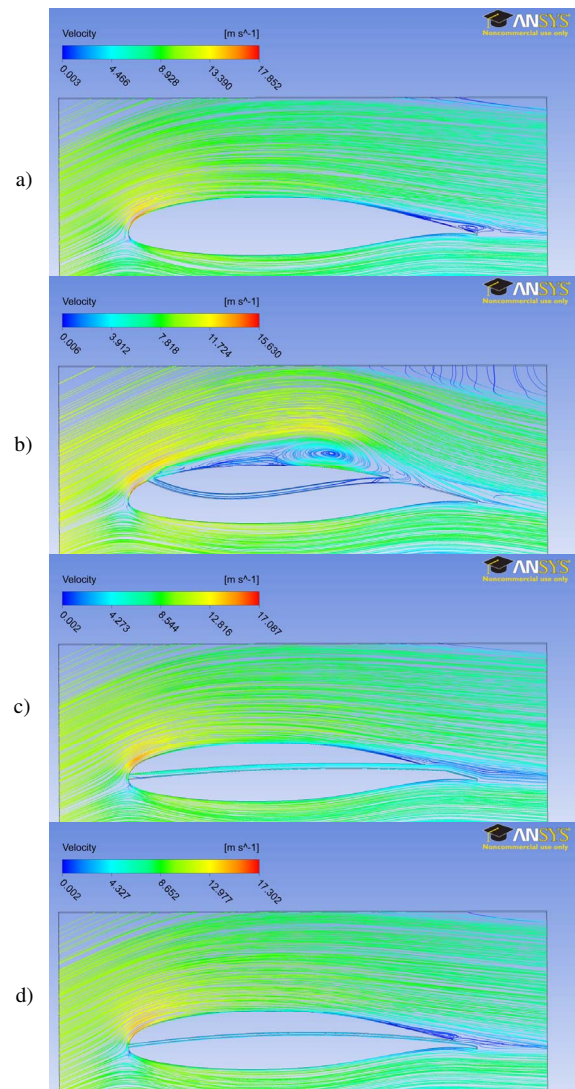


Figure 15. Velocity contours on streamlines for single blade configuration cases: a) baseline - airfoil with no secondary flow path; b) modified - flow inlet at 0.25c and exit at 0.75c; c) and d) flow inlet at leading edge and exit at .75c with thickness of 0.033 ft and 0.0166 ft respectively

This initial study provided promising results and validated that the concept of SFC did reduce flow separation as intended. Introducing the SFC system in the single airfoil model reduced the flow separation and recirculation. After analyzing all these secondary flow paths, it was determined that having a flow path before the separation region was crucial enough so that the flow does not further re-circulate. Also, having a very thin SFC does not remove enough mass. Hence, the flow path shown in Fig.15c) was selected as the SFC system to be investigated in the wind turbine

configuration. Figure 16 provides a close view of trailing edge and compares the default airfoil with the one with SFC selected.

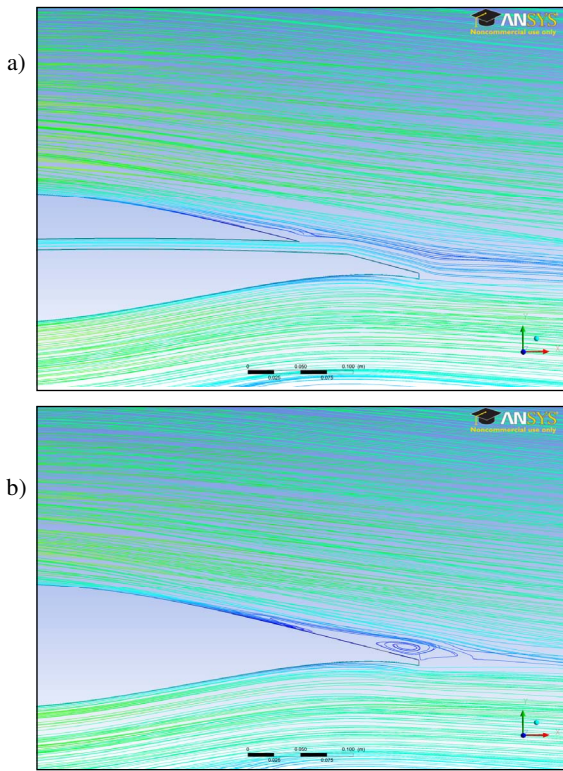


Figure 16. a) LS0417 with SFC in a single airfoil configuration b) LS0417 without SFC in a single airfoil

### Wind Turbine Simulations

The SFC found as best performing in a single airfoil configuration was used to alter the turbine blade geometry to allow comparison with the default turbine blade. Transient CFD simulations were used to mimic turbine’s rotation in a 1 degree increment until each blade described a full circle.

Figure 17 shows contour plots of velocity for the airfoil LS0417 with and without the secondary flow path, also providing a detail view of the retreating airfoil. Similar results, corresponding to NACA 8H12, are presented in Figure 18 to facilitate direct comparison between the two airfoils. A side by side comparison between LS0417 and NACA8H12 is illustrated in Figure 19 and 20, which show contour plots of velocity for five different apparent angles of attack as the turbine blades are advancing. In all the figures presented in this section, the incoming wind direction is from left to the right and the blades are rotating in counter clockwise direction.

As it can be seen in Figure17, the airfoil to the left has zero velocity near the leading edge indicating flow stagnation region, since the airfoil is retreating and opposing the flow direction. As can be seen, the inclusion of a SFC flow path

system, channels this flow in rotational motion to get rid of the zero velocity and separation region on the retreating airfoil.

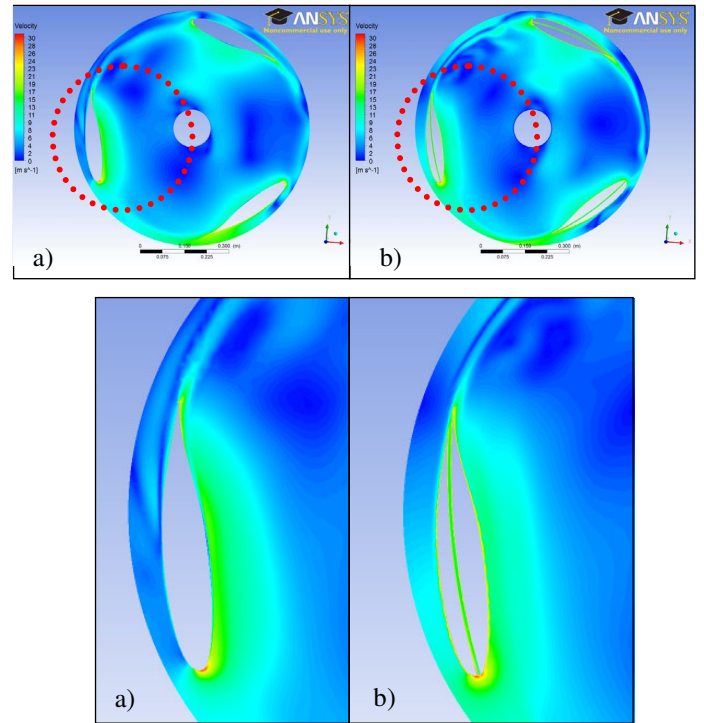


Figure 17. LS0417 velocity contour plots comparison between a) baseline and b)SFC; Top row shows inner rotating domain and a Detail view is shown on the bottom row

As can be seen in the figure above, the lower blade or the retreating airfoil does have a more streamlined flow pattern and the zero velocity regions over the top of the retreating airfoils are changed to a higher velocity flow region. For the advancing airfoil, the flow is modified, but it does not reduce flow separation for that particular apparent angle of attack. However, there is a significant improvement in the way air flows over the advancing blade due to the secondary flow system. Since, the airfoils are rotating at 700 rpm; there is interference between the airfoils. To address the issue of interference, the secondary flow path system needs to be optimized to take into consideration the effect interference has on the other airfoils.

As shown in Figure18, for this particular angular position of the blade, the secondary flow control system seems in general to be beneficial for NACA8H12; the flow becomes more streamlined, especially since it smoothes out the zero velocity patch on top of the advancing airfoil. However, from the figure shown on right side, first row, for the retreating airfoil, the flow is not very streamlined, and there is clear flow interference. The flow pattern around the airfoil is altered indeed, but the secondary flow path needs to be optimized for the retreating airfoils.

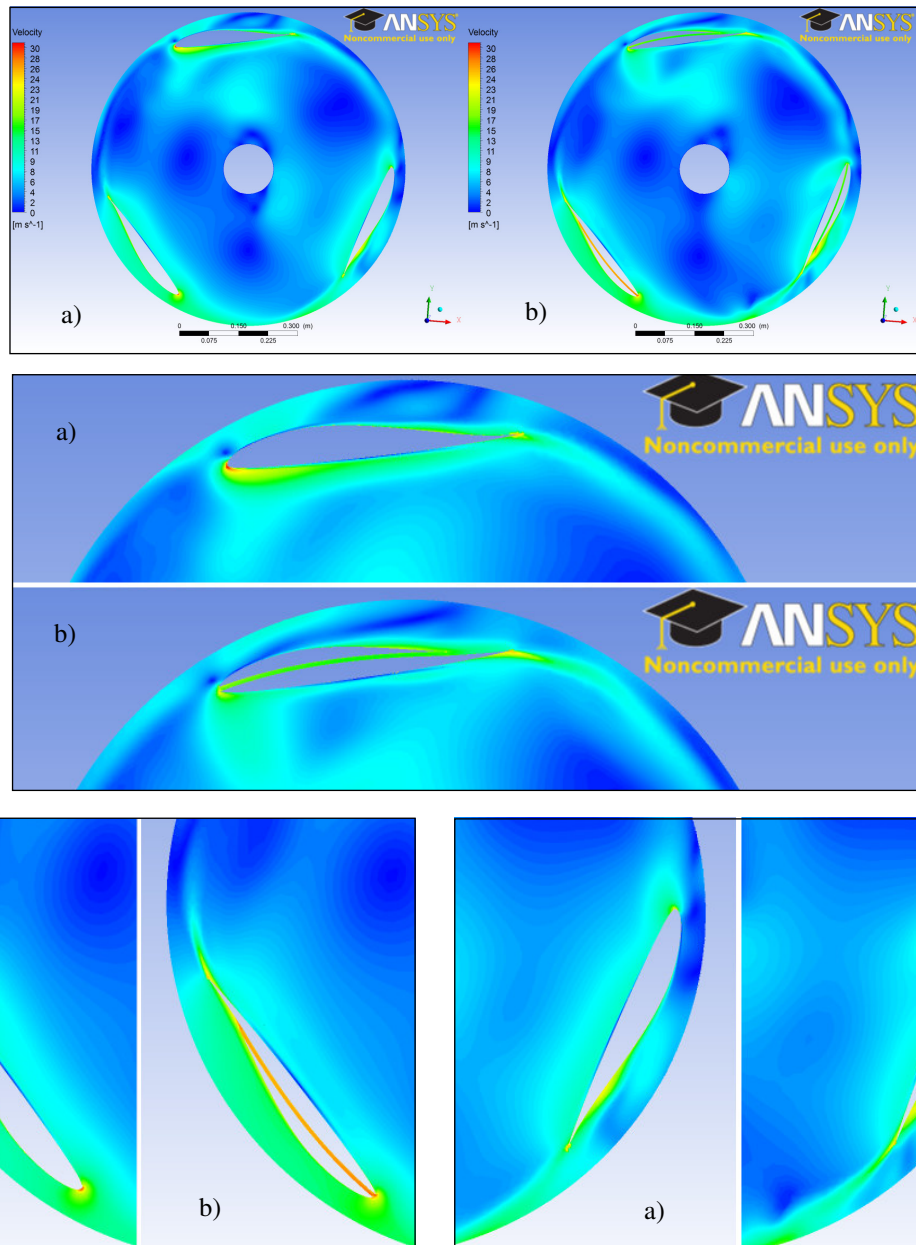
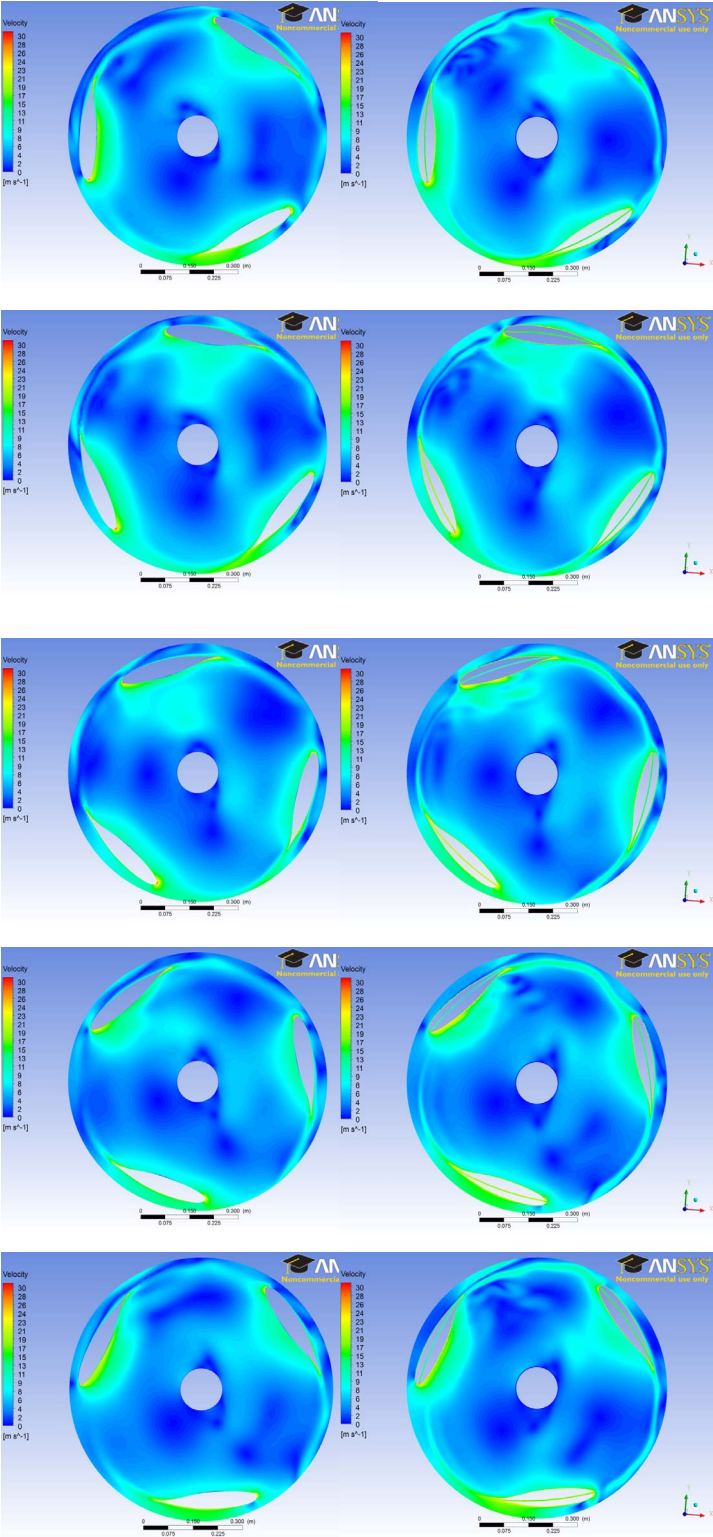


Figure 18. NACA8H12 - Contour plots of velocity a) without the SFC and b) with SFC; Top row shows inner rotating domain, the other two providing Detail view of the advancing and retreating blade

Figure 19 shows different time steps of the simulation for LS0417. The airfoil with SFC to the left, which is backtracking has an improved airflow, with reduced flow separation and stagnation regions on top of the airfoil. The SFC system has shown to smooth the velocity contours and provide a more streamlined flow. However, the SFC system does not necessarily correct the boundary layer separation at the same time for the other two blades remaining.

Based on direct comparison of Figures 19 and 20, one can conclude that LS0417 responds better to the introduction of the secondary flow control system, especially with flow

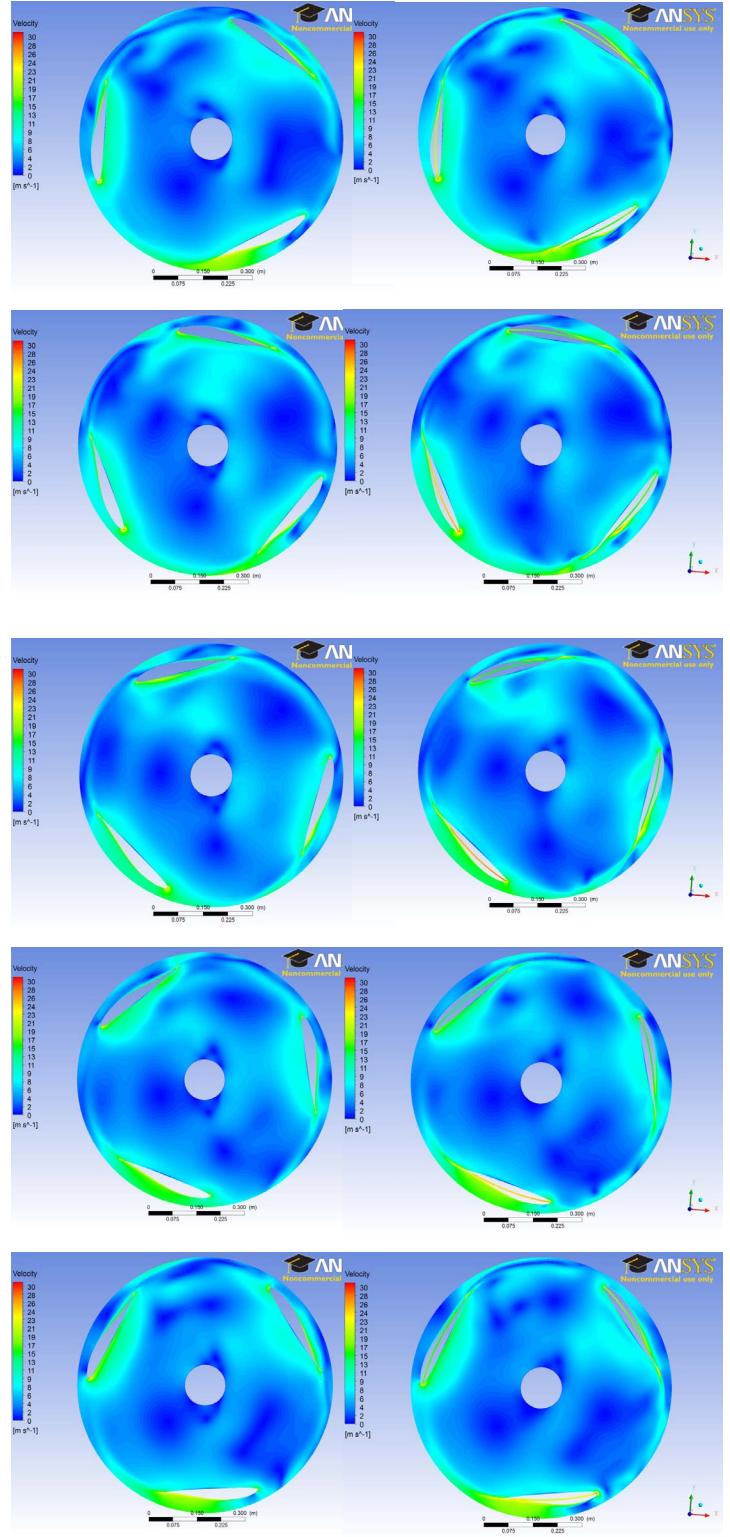
separation in retreating airfoils. NACA8H12 has certain apparent angles of attack which reduce the flow separation, whereas it also has certain angles where presence of secondary flow path worsens flow characteristics. This may be a consequence of the SFP geometry adopted in this study that was decided based on the investigation of flow characteristics of LS0417 only. Nevertheless, introduction of the secondary flow path system proved the ability to change the flow path passively, which makes this flow path system a promising passive flow control means.



a)

b)

Figure 19. LS0417–velocity contour plots comparison a) baseline and b) with SFC for different time steps as the blades rotate



a)

b)

Figure 20. NACA 8H12 - Contour plots of velocity a) baseline and b) with SFC for different time steps as the blades rotate

## CONCLUSION

The secondary-flow control system, proposed in this paper, works on the principle of mass removal and is intended to eliminate/reduce flow separation at different apparent angles of attack in a VAWT. CFD simulations were performed to ascertain the effects of a particular SFC in a vertical axis wind turbine configuration and validated the concept. Transient CFD simulations, where the inner domain containing the turbine's blades was advancing with 1 degree rotation per time step, were performed to replicate a full 360 degree rotation of the turbine, so that the entire range of apparent angles of attack in a VAWT is taken into account.

The results presented in this paper have showed that introducing a SFC system in a single airfoil configuration provides encouraging results, reducing the flow separation and flow recirculation at the trailing edge. The single airfoil simulation validated the location of the secondary flow path, which was then implemented in a 3-D configuration of a VAWT. In the wind turbine configuration, while the introduction of the secondary flow path system performs better in reducing flow separation in retreating airfoils of LS0417, the same geometry of secondary flow path system does not necessarily reduce the flow separation in NACA8H12. Still, the flow path is modified and controlled in both the airfoils due to the secondary flow path system. This result shows potential and opens up much more research possibilities in application of passive flow control in wind turbines, especially in Vertical axis wind turbines.

This study provided a good endorsement for using SFC system in wind turbines. Following this work, optimization needs to be done on the flow path configuration to better address the issue of flow interference due to the rotation.

## NOMENCLATURE

AOA – Angle of Attack

SFC – Secondary Flow Control

SFP – Secondary Flow Path

c – Chord

TSR – Tip-speed ratio

$\omega$  – Rotational speed of the rotor of the wind turbine, in rpm

v – Incoming wind velocity in m/s

## REFERENCES

1. Lee, C., Hong G., Ha, Q.P., and Mallinson, S.G., 2003. "A piezoelectrically actuated microsynthetic jet for active flow control." *Sensors and Actuators A*, 108:168-174.
2. Gad-el-Hak, M., 2000, Flow control: Passive, Active and Reactive Flow Management. *Cambridge University Press*, UK.
3. Lord, W.K., MacMartin, D.G., and Tillman, G., 2000. "Flow control opportunities in Gas Turbine Engines." AIAA Paper 2000-2234.
4. Schlitching, H., and Gersten, K., 2000. Boundary Layer theory, 8<sup>th</sup> edn. Springer.
5. Seifert, A., Greenblatt, D., and Wagnanski, I., 2004. "Active separation control: an overview of Reynolds and mach numbers effects." *Aerospace Science and Technology*: 569-582.
6. Han, Z., Zhang, K., Song, W., Qiao, Z., 2010. "Optimization of active flow control over an airfoil using a surrogate-management framework." *Journal of Aircraft*, 47(2): 603-612.
7. Huang, L., Huang, P.G., Lebeau, R.P., and Hauser, T., 2004. "Numerical study of blowing and suction control mechanism on NACA0012 airfoil." *Journal of Aircraft*, 41(5): 1005-1013.
8. Chandrasekhara, M.S., Tung.C., and Martin, P.B., 2004. "Aerodynamic Flow Control using a Variable Droop Leading Edge Airfoil." *RTO AVT Specialists' Meeting on "Enhancement of NATO Military Flight Vehicle Performance by Management of Interacting Boundary Layer Transition and Separation"*, Prague, Czech Republic.
9. Fish, F.E., and Lauder, G.V., 2006. "Passive and Active Flow Control by Swimming Fishes and Mammals." *Annual Review of Fluid Mechanics*, 38: 193-224.
10. Anderson, J.D., 2000. Introduction to flight. 4th edn., New York :McGraw-Hill.
11. Favier, J., Dauptain, A., Basso, D., and Bottaro, A., 2009. "Passive separation control using a self-adaptive hairy coating." *Journal of Fluid Mechanics*, 627: 451-483.
12. Bruneau, C., Mortazavi, I., 2008. "Numerical modeling and passive flow control using porous media." *Computers & Fluids*, 37(5): 488-498.
13. Bridges, D., 2007. "Early flight-test and other boundary layer research at Mississippi State 1949-1960." *Journal of Aircraft* 44(5): 1635-1652.
14. Johnson, S.J., van Dam, C.P., and Berg, D.E., 2008. "Active Load Control Techniques for Wind Turbines." *Sandia Report*, SAND2008-4809.
15. Buhl, T., Gauuna, M., and Bak, C., 2005. "Potential Load Reduction Using Airfoils with Variable Trailing Edge Geometry." *Journal of Solar Energy Engineering*, 127(4): 503-516.
16. Basualdo, S., 2005, "Load alleviation on wind turbine blades using variable airfoil geometry." *Wind Engineering*, 29(2): 169-182.
17. van Dam, C. P., Chow, R., Zayas, J.R., and Berg, D.E., 2007, "Computational Investigations of Small Deploying Tabs and Flaps for Aerodynamic Load Control " *J. Phys.: Conf. Ser.* 75: 012027.
18. Lackner, M.A., and van Kuik, G., 2010. "A comparison of smart rotor control approaches using trailing edge flaps and individual pitch control." *Wind Energy*, 13(2-3): 117-134.
19. Troldborg, N., 2005, "Computational study of the Risø-B1-18 airfoil with a hinged flap providing variable trailing edge geometry." *Wind Engineering*; 29: 89-113.

20. van Wingerden, J., Hulskamp, A., Barlas, T., Marrant, B., van Kuik, G., Molenaar, D., Verhaegen, M., 2008, "On the proof of concept of a 'smart' wind turbine blade for load alleviation." *Wind Energy*, 11: 265–280.
21. Bossanyi, E., 2003. "Individual blade pitch control for load reduction." *Wind Energy*, 6: 119–128.
22. McCoy, T., Griffin, D., 2006. "Active control of rotor aerodynamics and geometry: status, methods, and preliminary results." *44th AIAA Aerospace Science Meeting and Exhibit*, Reno, NV, USA, 2006; AIAA-2006-0605.
23. Giguere, P., and M. Selig, 1999, "Design of a Tapered and Twisted Blade for the NREL Combined Experiment Rotor." *NREL/SR 500-26173*, National Renewable Energy Laboratory, Golden, CO.
24. Joncas, S., Bergsma, O., and Beukers, A., 2005, "Power Regulation and Optimization of Offshore Wind Turbines through Trailing Edge Flap Control," *Wind Energy Symposium*, Jan. 2005, Reno, Nevada, USA. AIAA Paper 2005-0394.
25. Johnson, S.J., Baker, J.P., van Dam, C.P., and Berg, D.E., 2010. "An overview of active load control techniques for wind turbines with an emphasis on microtabs." *Wind Energy*, 13:239-253.
26. Untaroiu A., Barker L.R., Wood H.G., Ribando R.J., Allaire P.E., 2010, "Numerical Investigation of Aerodynamic Performance of a three-bladed Vertical Axis Wind Turbine", *Proceedings of the ASME International Mechanical Engineering Congress and Exposition 2010*, Paper no. IMECE2010-39267.
27. Colson&Associates, 1995, Avian interaction with wind facilities: A summary, *American Wind Energy Association*.
28. US Patent: US2136403A, 1935.